COMMUNICATION

Self-Assembly Supramolecular Polymer by Anti-Electrostatic Anion-Anion and Halogen Bonding Interactions

Received 00th January 20xx,
Accepted 00th January 20xx

DOI: 10.1039/x0xx00000x

Fabiola Zapata,[a*] Lidia González,[a] Adolfo Bastida,[b] Delia Bautista,[c] Antonio Caballero.[a*]

We report here the generation of a self-assembly supramolecular polymer in which the cooperative action of anti-electrostatic anion-anion and halogen-bonding interactions serve as a powerful driven force to form large supramolecular polymers. DOSY-NMR, DLS, TEM, SEM and X-ray experiments evidence the formation of supramolecular structures in solution and solid state.

Coulomb's Law, which is probably one of the first principles taught to science students, states that two charged species will attract or repel each other if they have opposite or identical signs respectively due to electrostatic forces[1] and therefore, two or more cations or anions will maximize their distances to minimize the electrostatic repulsions. In 2014 Weinholds theoretically characterized a surprising new class of H-bonded complexes between ions of like charge using ab initio and hybrid density functional techniques.[2] These results opened a very interesting discussion about the existence of anion-anion dimers[3] where some authors affirm that such aggregates can be stabilized by attractive electrostatic interactions by hydrogen bonds that balance electrostatic repulsion.[4] A recent survey of the Cambridge Structural Database[5] indicates that the existence of anion-anion aggregates is not rare in the solid state but surprisingly this interaction has not received much attention in the context of crystal engineering.[6] Some of the remarkable examples described in the literature in solid state are the aggregation of hydrogensulfate[7] and dihydrogenphosphate anions,[8] stabilized by organic ligands, into a wide variety of different structures.

[a.] *Departamento de Química Orgánica, Universidad de Murcia, Campus de Espinardo, 30100 Murcia, Spain. E-mail: antocaba@um.es, fazafer@um.es*
[b.] *Departamento de Química Física, Universidad de Murcia, Campus de Espinardo, 30100 Murcia, Spain.*
[c.] *Servicio de Apoyo a la Investigación, Universidad de Murcia, Campus de Espinardo, E-30071 Murcia, Spain*
† Footnotes relating to the title and/or authors should appear here.
Electronic Supplementary Information (ESI) available Experimental procedures, synthesis, NMR experiments, thermodynamic model analysis and X-ray data. See DOI: 10.1039/x0xx00000x

The idea that anions can be bounded to each other in solution is practically underexplored[9] and only a few acyclic, monocyclic, bicyclic and tricyclic anion receptors offer a way to stabilize anionic aggregates in solution using a variety of noncovalent interactions, such a hydrogen bonding, electrostatic interactions and anion-π.[10]

The construction of supramolecular polymers induced by anion-anion interactions is quite rare and only a few examples have been described. In 2010 Sessler reported the formation of a self-assembled supramolecular pseudo-oligorotaxanes where terephthalate anions were bonded each other stabilised by an imidazolium based macrocycle[11]. More recently Flood has reported the formation of supramolecular polymer induced by the dimerization of difunctional phosphonate monomers in which each anion is stabilized by a cyanostar macrocycle.[12]

Among non-covalent interactions used to stabilize anionic aggregates in solution, halogen bonding remains almost unexplored. Halogen bonding is within the family of the σ-hole interactions where the attraction for negative species is caused by the anisotropic distribution of the electron density in the halogen atom which originates a positive (σ-hole) and negative (σ-lump) regions of electron density.[13] In fact, halogen bonding is considered as an excellent alternative to hydrogen bonding in supramolecular chemistry, nevertheless, halogen bond is still a developing and relatively immature research field.[14]

We have recently reported[15] the utilization of a halogen bond donor in the formation of a self-assembly supramolecular polymer induced by SO_4^{2-} anions, where two linear chains are interpenetrated each other. We also detected strong evidences of the formation of supramolecular polymers induced by the presence of $H_2PO_4^-$ anion, but unfortunately no structural information of the supramolecular polymer induced by $H_2PO_4^-$ anions was obtained.

Motivated by the ability of the $H_2PO_4^-$ anions to form aggregates we have decided to change the halogen bond donor in order to explore the possibility of the formation of supramolecular polymers by the aggregation of $H_2PO_4^-$ anions. As a consequence of our research, we describe here the

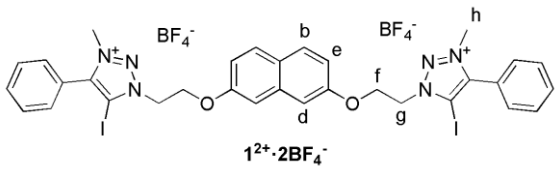

Fig. 1 Structure of the halogen bond donor $\mathbf{1^{2+}\cdot 2BF_4^-}$.

formation of a self-assembly supramolecular polymer in which non-common anti-electrostatic anion-anion interactions, stabilized with halogen bond donor, serve as a powerful driven force to form long 1D supramolecular polymers in solution.

The halogen bond donor $\mathbf{1^{2+}\cdot 2BF_4^-}$, used as organic building block, contain two iodotriazolium rings as anion binding sites, substituted in the C-4 with a benzene ring and naphthalene as spacer (Fig. 1).

The ability of the halogen bond donor $\mathbf{1^{2+}\cdot 2BF_4^-}$ to form supramolecular polymers with the presence of $H_2PO_4^-$ anions as tetrabutylammonium salts was initially investigated using ^{1}H NMR titration experiments through the addition of aliquots of the anion to solutions of the halogen bond donor $\mathbf{1^{2+}\cdot 2BF_4^-}$ in the solvent mixture CD_3CN/CD_3OD 9:1. The first evidences of the formation of supramolecular polymers were detected by analysing the titration profiles obtained by ^{1}H NMR following the signal of the naphthalene H_d protons (Fig. 2a) in which the addition of up to 1 equiv. of $H_2PO_4^-$ did not promote remarkable changes in the ^{1}H NMR spectrum of the monomer, but subsequent additions of $H_2PO_4^-$ anions promoted a noticeable downfield shift of the naphthalene H_d ($\Delta\delta$ = 0.30 ppm). This behaviour is indicative that a polymerization process is taking place rather than the typical recognition event. The study of the change of some measured data sensible to the formation of polymerization processes reveal that the shape of the experimental curves are qualitative different from those obtained for simple association.[16] In addition, the H_g protons (-N-CH_2-) are also downfield shifted by the presence of $H_2PO_4^-$ anions ($\Delta\delta$ = 0.16 ppm) following a similar trend (Fig. 2b and Electronic Supplementary Information).

The reversibility of the supramolecular polymerization-depolymerization process of $\mathbf{1^{2+}\cdot 2BF_4^-}$ was investigated by ^{1}H-NMR spectroscopy by addition of Zn^{2+} cations which can sequester the $H_2PO_4^-$ from the supramolecular polymer. Thus, after addition of Zn^{2+} the ^{1}H-NMR spectrum of the monomer was recovered. Several polymerization-depolymerization cycles were carried out by the sequential addition of $H_2PO_4^-$ and Zn^{2+} ions to a solution of the compound $\mathbf{1^{2+}\cdot 2BF_4^-}$.

We have reported recently a chemical model which uses the ^{1}H NMR titration data to describe quantitatively the thermodynamic of the polymerization process.[17] This model allows us to calculate the equilibrium constants K_N and K_E corresponding to the nucleation and elongation steps respectively. The thermodynamic model is also able to estimate the anion/monomer stoichiometry in the polymer (see Electronic Supplementary Information). The theoretical curve fits well the experimental data (Fig. 2a) providing a theoretical anion/monomer ratio of 1.84. The calculated values of K_N and K_E when the value of n was fixed to 2 are $K_N = 6.37\cdot10^5$ M^{-2} and

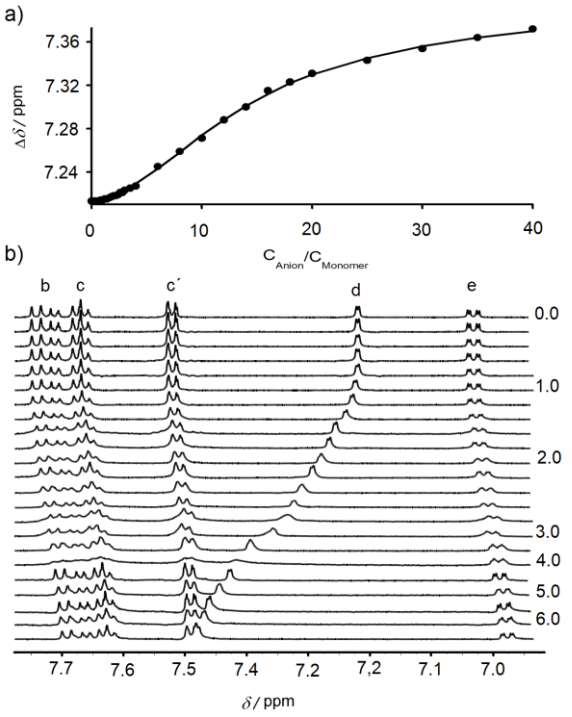

Fig. 2 a) Changes in the chemical shift of the naphthalene H_d proton of the monomer $\mathbf{1^{2+}\cdot 2BF_4^-}$ upon addition of increasing amounts $H_2PO_4^-$ anions. Points represent experimental data and the continuous line represents the fit to the model. b) ^{1}H NMR spectral changes observed in $\mathbf{1^{2+}\cdot 2BF_4^-}$ in CD_3CN/CD_3OD (9/1, v/v) during the addition of up to 6.5 equiv. of $H_2PO_4^-$.

$K_E = 1.28\cdot10^9$ M^{-3}. Although both equilibrium constants have different units, we can estimate their similarity using the value of C_A as a conversion factor. In that case, we obtain values of K_N and $K_E\cdot C_A$ with similar order of magnitude suggesting that the growth of the supramolecular polymer follows an isodesmic mechanism.[18]

In order to get additional evidences of the formation of the self-assembly supramolecular polymers in solution, diffusion NMR (DOSY NMR) and dynamic light scattering (DLS) studies were carried out.

One of the simplest experiments to detect the formation of self-assembled supramolecular polymers or other type of aggregates in solution is the obtention of the diffusion coefficient (D). The generation of this type of self-assembled material usually cause a remarkable decrease in the diffusion coefficient value compared with the monomer. The results obtained by DOSY NMR show that the diffusion coefficient values of $\mathbf{1^{2+}\cdot 2BF_4^-}$ are basically independent of the concentration of the monomer (Figure 2a) as expected if neither polymerization nor aggregation of the monomer are present.

The addition of $H_2PO_4^-$ anions reduces significantly the diffusion coefficients (between -15% and -25%) being this decrease more pronounced as the initial concentration of the monomer increases as expected from the formation of larger and larger supramolecular species. (Fig. 3a).

The size of the supramolecular polymer at different concentrations was obtained by DLS measurements in CH_3CN. The hydrodynamic diameter is of an equivalent sphere having the same diffusion coefficient as the measured one, although

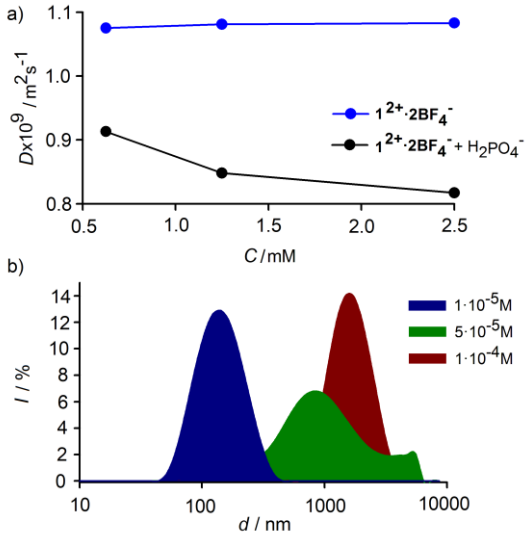

Fig. 3 a) Diffusion coefficient values of $\mathbf{1^{2+}{\cdot}2BF_4^-}$ (blue line) and $\mathbf{1^{2+}{\cdot}2BF_4^-}$ with the addition of $H_2PO_4^-$ anions (black line) in CD_3CN/CD_3OD (9/1, v/v). b) Distribution of the hydrodynamic diameter of $\mathbf{1^{2+}{\cdot}2\ H_2PO_4^-}$ as measured though DLS at c = 0.1 (red), 0.05 (green), and 0.01 mM (blue) in CH_3CN at 25 °C.

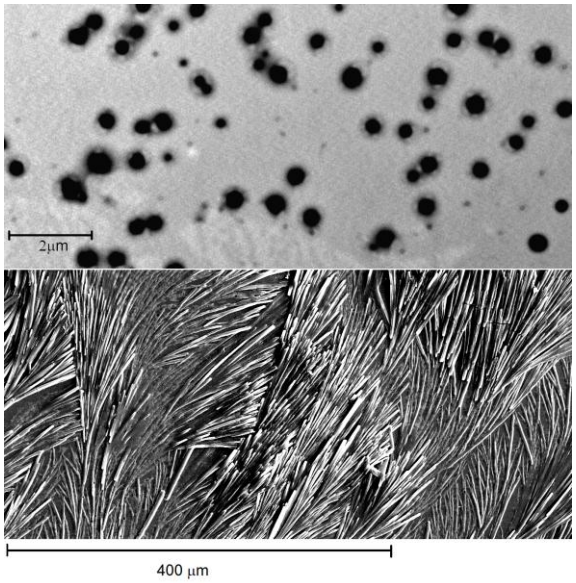

Fig. 4 TEM (top) and SEM (bottom) images of the supramolecular polymer formed upon the addition of $H_2PO_4^-$ to a solution of receptor $\mathbf{1^{2+}{\cdot}2BF_4^-}$.

the shape of the aggregates may differ from a sphere. The values of the hydrodynamic diameter of the specie formed after the addition of $H_2PO_4^-$ to a solution of $\mathbf{1^{2+}{\cdot}2BF_4^-}$ decrease when the concentration of the monomer also decrease, so that, the largest supramolecular polymer was measured at c = $1.0{\cdot}10^{-4}$ M with d = 1186 nm, while the shortest one was measured at c = $1.0{\cdot}10^{-5}$ M d = 128 nm (Fig. 3b). The large supramolecular polymers detected by DLS experiments (CH_3CN) are consistent with the modest decrease of the diffusion coefficient obtained by DOSY NMR experiments (CD_3OD 10%) because of the presence of methanol which is a very competitive solvent in the formation of anion induced supramolecular polymer.

Transmission Electron Microscopy (TEM) images of the supramolecular polymer prepared immediately upon the addition of $H_2PO_4^-$ to a solution of receptor $\mathbf{1^{2+}{\cdot}2BF_4^-}$ in CH_3CN allowed to get structural information about the supramolecular polymer at the level of its formation. The supramolecular polymer exhibits the generation of nanoobjects with spherical morphology, presenting relatively uniform sizes around 0.5 μm (Fig 4 top).

The crystal-growing process was also studied by Scanning Electron Microscopy (SEM) and the images revealed the formation of thousands of highly directional 1D crystals, the long fibers probably grow from the spheres observed in the TEM images. The widths of the fibers were very uniform around 2 μm. Due to the overlapping of the fibers, it was not possible an accurate estimation of their average length (Fig. 4 bottom). Nevertheless, it is not difficult to observe fibers around 1 mm long.

Single crystals,[19] suitable for X-ray diffraction structural analysis, were obtained for the supramolecular polymer $\mathbf{1^{2+}{\cdot}2H_2PO_4^-}$[20] by the vapor diffusion of diethyl ether into a solution of the supramolecular polymer $\mathbf{1^{2+}{\cdot}2H_2PO_4^-}$ in CH_3CN/CH_3OH (9:1, v/v). The solid-state structure shows the formation of a supramolecular linear chain of $H_2PO_4^-$ anions bond each other by four different hydrogen bonding interactions (-P-O···HO-P- 59-63% of sum of vdW). One of the iodotriazolium of the organic monomer $\mathbf{1^{2+}}$ forms strong halogen-bonding interactions with the $H_2PO_4^-$ anion (C-I···O-P- 80% of sum of vdW), while the other iodotriazolium weakly interacts with one of the carbon of the naphthalene ring of other organic monomer $\mathbf{1^{2+}}$ (C-I···C-C 99% of sum of vdW) (Fig. 5).

In summary, we have reported here a new halogen bonding anion receptor bearing naphthalene ring as a central core

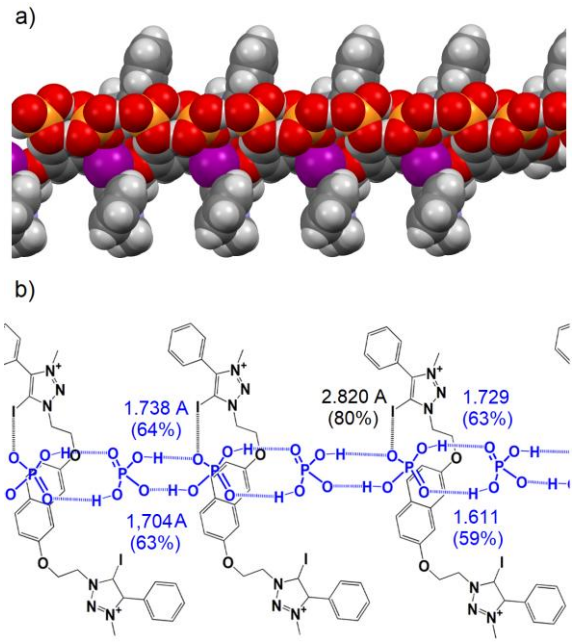

Fig. 5 a) Space-filling representation of the X-ray structure of the supramolecular polymer $\mathbf{1^{2+}{\cdot}2H_2PO_4^-}$. Color scheme: gray = carbon, blue = nitrogen, purple = iodine, red = oxygen, orange = phosphorus and white = hydrogen. b) Schematic representation of the supramolecular polymer $\mathbf{1^{2+}{\cdot}2H_2PO_4^-}$ showing the halogen- (black) and hydrogen bonding (blue) interactions. Distances are in angstroms, and those in brackets are the ΣrvdW.

decorated with two arms containing iodotriazolium rings as anion binding sites which is able to form a self-assembly supramolecular polymers in which the cooperative action of non-common anti-electrostatic anion-anion and halogen bonding interactions serve as a powerful driven force to form a long supramolecular polymers in solution. The evidences of the formation of supramolecular polymers in solution came from DOSY NMR and DLS experiments where an important decrease in the diffusion coefficient, compared with the monomer, and large supramolecular structures were detected in solution respectively. ^{1}H NMR studies demonstrated the reversibility of the polymerization−depolymerization process. The nucleation K_N and the elongation K_E constants were obtained from the NMR titration experiments and indicate that the growth of the supramolecular polymer follows an isodesmic mechanism. Scanning electron microscopy studies revealed the formation of long 1D needle-like fibers. The X-ray structure of the supramolecular polymer shows the formation of a supramolecular linear chain of $H_2PO_4^-$ anions bond each other by hydrogen bonding interactions. The chain of anions is stabilized by the organic monomer $\mathbf{1^{2+}}$ by the formation of strong halogen-bonding interactions with the $H_2PO_4^-$ anions.

We thank the government of the Spain Agencia Estatal de Investigación (AEI) and Fondo Europeo de Desarrollo Regional (FEDER, UE) projects CTQ2017-86775-P CTQ2016-79345-P and RED2018-102331-T and Fundación Séneca Región de Murcia (CARM) projects 20819/PI/18 and 20789/PI/18 for financial support. L.G. and F.Z. also acknowledges to the government of Spain and the University of Murcia for a FPI predoctoral and a postdoctoral grant respectively.

Conflicts of interest

There are no conflicts to declare.

Notes and references

1 C. A. Coulomb, Mémoires de l'Académie Royale des Sciences, 1788, 569 – 577.
2 F. Weinhold, R. A. Klein, *Angew. Chem. Int. Ed.*, 2014, **53**, 11214 – 11217.
3 *(a)* G. Frenking, G. F. Caramori, *Angew. Chem. Int. Ed.*, 2015, **54**, 2596 – 2599; *(b)* F. Weinhold, R. A. Klein, *Angew. Chem. Int. Ed.*, 2015, **54**, 2600 – 2602; *(c)* I. Mata, E. Molins, I. Alkorta, E. Espinosa, *J. Phys. Chem. A*, 2015, **119**, 183 – 194; *(d)* A. Knorr, P. Stange, K. Fumino, F. Weinhold, R. Ludwig, *ChemPhysChem*, 2016, **17**, 458 – 462.
4 *(a)* I. Mata, I. Alkorta, E. Molins and E. Espinosa, *ChemPhysChem*, 2012, **13**, 1421–1424; *(b)* I. Mata, I. Alkorta, E. Molins, E. Espinosa, *Chem. Phys. Lett.*, 2013, **555**, 106–109; *(c)* I. Mata, E. Molins, I. Alkorta, E. Espinosa, *J. Phys. Chem. A*, 2015, **119**, 183–194.
5 C. R. Groom, I. J. Bruno, M. P. Lightfoot and S. C. Ward, Acta Crystallogr., 2016, **B72**, 171–179.
6 D. A. Cullen, M. G. Gardiner, N. G. White, *Chem. Commun*., 2019, **55**, 12020–12023-
7 *(a)* P. Colomban, M. Pham-Thi, A. Novak, *Solid State Ionics*, 1987, **24**, 193–203; *(b)* M. Malchus, M. Jansen, *Acta Crystallogr., Sect. B: Struct. Sci*., 1988, **54**, 494–502; *(c)* P. H. Toma, M. P. Kelley, T. B. Borchardt, S. R. Byrn, B. Kahr, *Chem. Mater*., 1994, **6**, 1317–1324; *(d)* M. E. Light, P. A. Gale, M. B. Hursthouse, *Acta Crystallogr., Sect. E: Struct. Rep*. Online, 2001, **57**, 705–706; *(e)* R. Custelcean, N. J. Williams, C. A. Seipp, *Angew. Chem. Int. Ed.*, 2015, **54**, 10525–10529; *(f)* M. N. Hoque, U. Manna, G. Das, *Supramol. Chem*., 2016, **28**, 284–292.
8 *(a)* D. M. Rudkevich, W. Verboom, Z. Brzozka, M. J. Palys, W. P. R. V. Stauthamer, G. J. van Hummel, S. M. Franken, S. Harkema, J. F. J. Engbersen, D. N. Reinhoudt, *J. Am. Chem. Soc.*, 1994, **116**, 4341–4351; *(b)* P. S. Lakshminarayanan, I. Ravikumar, E. Suresh, P. Ghosh, *Chem. Commun*., 2007, 5214–5216; *(c)* J. Ju, M. Park, J. M. Suk, M. S. Lah, K.-S. Jeong, *Chem. Commun*., 2008, 3546–3548; *(d)* P. Dydio, T. Zielínski, J. Jurczak, *Org. Lett.*, 2010, **12**, 1076–1078; *(e)* F. A. Cotton, B. A. Frenz, D. L. Hunter, *Acta Crystallogr., Sect. B: Struct. Crystallogr. Cryst. Chem.*, 1975, **31**, 302–304; *(f)* N. Ohama, M. Machida, T. Nakamura, Y. Kunifuji, *Acta Crystallogr., Sect. C: Cryst. Struct. Commun.*, 1987, **43**, 962–964; *(g)* J. M. Karle, I. L. Karle, *Acta Crystallogr., Sect. C: Cryst. Struct. Commun.*, 1988, **44**, 1605–1608; *(h)* M. E. Light, S. Camiolo, P. A. Gale, M. B. Hursthouse, Acta Crystallogr., *Sect. E: Struct. Rep. Online*, 2001, **57**, 727–729; *(i)* V. Amendola, M. Boiocchi, D. Esteban-Gómez, L. Fabbrizzi, E. Monzani, *Org. Biomol. Chem.*, 2005, **3**, 2632–2639; (j) B. Lou, X. Guo and Q. Lin, *J. Chem. Crystallogr*., 2009, **39**, 469–473; (k) A. Rajbanshi, S. Wan and R. Custelcean, *Cryst. Growth Des*., 2013, **13**, 2233–2237; *(l)* B. Wu, C. Huo, S. Li, Y. Zhao, X.-J. Yang, *Z. Anorg. Allg. Chem*., 2015, **641**, 1786–1791; (m) M. A. Hossain, M. Isiklan, A. Pramanik, M. A. Saeed, F. R. Fronczek, *Cryst. Growth Des*., 2012, **12**, 567–571; *(n)* V. Blazek, K. Molcanov, K. Mlinaric-Majerski, B. Kojic- Prodic, N. Basaric, *Tetrahedron*, 2013, **69**, 517–526.
9 E. M. Fatila, E. B. Twum, A. Sengupta, M. Pink, J. A. Karty, K. Raghavachari, A. H. Flood, *Angew. Chem. Int. Ed*. 2016, **55**, 14057–14062.
10 Q. He, P. Tu, J. L. Sessler, *Chem,* 2018, **4**, 46–93.
11 H-Y. Gong, B. M. Rambo, E. Karnas, V. M. Lynch, J. L. Sessler, *Nat. Chem.,* 2010, **2**, 406-409.
12 *(a)* W. Zhao, B. Qiao, J. Tropp, M. Pink, J. D. Azoulay, Amar H. Flood, *J. Am. Chem. Soc*. 2019, **141**, 4980−4989; *(b)* W. Zhao, J. Tropp, B. Qiao, M. Pink, J. D. Azoulay, A. H. Flood, *J. Am. Chem. Soc.* 2020, **142**, 2579−2591
13 *(a)* P. Politzer, J. S. Murray, *Crystals,* 2017, **7**, 212 – 226; *(b)* J. S. Murray, P. Lane, T. Clark, K. E. Riley, P. Politzer, *J. Mol. Model.* 2012, **18**, 541–548.
14 *(a)* G. Cavallo, P. Metrangolo, R. Milani, T. Pilati, A. Primagi, G. Resnati, G. Terraneo, *Chem. Rev.*, 2016, **116**, 2478; *(b)* L. C. Gilday, S. W. Robinson, T. A. Barendt, M. J. Langton, B. R. Mullaney, P. D. Beer, *Chem. Rev.*, 2015, **115**, 7118–7195.
15 F. Zapata, L. González, A. Caballero, A. Bastida, D. Bautista, and P. Molina. *J. Am. Chem. Soc.*, 2018, **140**, 2041.
16 *(a)* A. Sorrenti, J. Leira-Iglesias, A. J. Markvoort, T. F. A de Greef, T. M. Hermans, *Chem. Soc. Rev*., 2017, **46**, 5476–5490; *(b)* J. van Herrikhuyzen, A. Syamakumari, A. Schenning, E. Meijer, *J. Am. Chem. Soc*. 2004, **126**, 10021–10027.
17 P. Sabater, F. Zapata, A. Bastida, A. Caballero, *Org. Biomol. Chem.*, 2020, DOI: 10.1039/d0ob00258e
18 *(a)* D. Zhao, J. Moore, *Org. Biomol. Chem*. 2003, **1**, 3471; *(b)* A. Sorrenti, J. Leira-Iglesias, A. J. Markvoort, T. F. A. de Greef, T. M. Hermans, *Chem. Soc. Rev.,* 2017, **46**, 5476–5490.
19 The crystal used for the X-Ray diffraction analysis was similar to the fibers showed in the SEM images
20 CCDC 1989705 contains the supplementary crystallographic data for this paper. These data are available free of charge from The Cambridge Crystallographic Data Centre.

